

Analysis for Effects of Temperature Rise of PV Modules upon Driving Distance of Vehicle Integrated Photovoltaic Electric Vehicles

Masafumi Yamaguchi^{1*}, Yasuyuki Ota², Taizo Masuda³, Christian Thiel⁴, Anastasios Tsakalidis⁴, Arnulf Jaeger-Waldau⁴, Kenji Araki², Kensuke Nishioka², Tatsuya Takamoto⁵, Takashi Nakado⁶, Kazumi Yamada⁶, Tsutomu Tanimoto⁷, Yosuke Tomita⁷, Yusuke Zushi⁷, Kenichi Okumura³, Takashi Mabuchi³, Akinori Satou³, Kyotaro Nakamura¹, Ryo Ozaki¹, Nobuaki Kojima¹, Yoshio Ohshita¹

¹Toyota Technological Institute, Nagoya, Japan

²Faculty of Engineering, Miyazaki University, Miyazaki, Japan

³Toyota Motor Corporation, Susono, Japan

⁴European Commission—Joint Research Centre, Ispra, Italy

⁵Sharp Corporation, Nara, Japan

⁶Toyota Motor Corporation, Toyota, Japan

⁷Nissan Motor Corporation, Yokosuka, Japan

Email: *masafumi@toyota-ti.ac.jp

How to cite this paper: Yamaguchi, M., Ota, Y., Masuda, T., Thiel, C., Tsakalidis, A., Jaeger-Waldau, A., Araki, K., Nishioka, K., Takamoto, T., Nakado, T., Yamada, K., Tanimoto, T., Tomita, Y., Zushi, Y., Okumura, K., Mabuchi, T., Satou, A., Nakamura, K., Ozaki, R., Kojima, N. and Ohshita, Y. (2024) Analysis for Effects of Temperature Rise of PV Modules upon Driving Distance of Vehicle Integrated Photovoltaic Electric Vehicles. *Energy and Power Engineering*, 16, 131-150. <https://doi.org/10.4236/epe.2024.164007>

Received: February 22, 2024

Accepted: April 5, 2024

Published: April 8, 2024

Copyright © 2024 by author(s) and Scientific Research Publishing Inc. This work is licensed under the Creative Commons Attribution International License (CC BY 4.0).

<http://creativecommons.org/licenses/by/4.0/>



Open Access

Abstract

The development of vehicle integrated photovoltaics-powered electric vehicles (VIPV-EV) significantly reduces CO₂ emissions from the transport sector to realize a decarbonized society. Although long-distance driving of VIPV-EV without electricity charging is expected in sunny regions, driving distance of VIPV-EV is affected by climate conditions such as solar irradiation and temperature rise of PV modules. In this paper, detailed analytical results for effects of climate conditions such as solar irradiation and temperature rise of PV modules upon driving distance of the VIPV-EV were presented by using test data for Toyota Prius and Nissan Van demonstration cars installed with high-efficiency InGaP/GaAs/InGaAs 3-junction solar cell modules with a module efficiency of more than 30%. The temperature rise of some PV modules studied in this study was shown to be expressed by some coefficients related to solar irradiation, wind speed and radiative cooling. The potential of VIPV-EV to be deployed in 10 major cities was also analyzed. Although sunshine cities such as Phoenix show the high reduction ratio of driving range with 17% due to temperature rise of VIPV modules, populous cities such as Tokyo show low reduction ratio of 9%. It was also shown in this paper that the difference between the driving distance of VIPV-EV driving in

the morning and the afternoon is due to PV modules' radiative cooling. In addition, the importance of heat dissipation of PV modules and the development of high-efficiency PV modules with better temperature coefficients was suggested in order to expand driving range of VIPV-EV. The effects of air-conditioner usage and partial shading in addition to the effects of temperature rise of VIPV modules were suggested as the other power losses of VIPV-EV.

Keywords

Vehicle Integrated Photovoltaics (VIPV), VIPV-Powered Electric Vehicles, Driving Distance, PV Modules, Solar Irradiation, Temperature Rise, Radiative Cooling

1. Introduction

Developing a vehicle powered by an onboard photovoltaics (PV) module [1] [2] [3] is desirable and essential for reducing CO₂ emissions with more than 50% reduction [4]. Although a daily driving distance of 26.6 km/day has been estimated for the Toyota Prius demonstration car installed with a high-efficiency PV module with a module efficiency of more than 30% in our previous paper [5], practical cruise range of VIPV (vehicle-integrated)-powered electric vehicles (VIPV-EV) is shown to be lower (17.0 km/day [6]) than the estimated values due to some losses such as temperature rise of PV modules, partial shading due to trees and buildings and so forth. The results suggest that various loss analysis of PV modules such as effects of temperature rise, partial shading, usage of air-conditioner and so forth is essential to guide the development of VIPV modules to spread the VIPV- powered electric passenger cars.

Brief analytical results for the effects of solar irradiation and temperature rise upon VIPV-EV have been presented at the 50th IEEE Photovoltaic Specialists Conference [7]. This paper presents detailed analytical results for the effects of solar irradiation and temperature rise of PV modules upon driving distance of VIPV-EV by using our test data for Toyota Prius and Nissan Van demonstration cars. The temperature rise of some PV modules studied in this study is shown to be expressed by some coefficients related to solar irradiation, wind speed and radiative cooling. Analytical results for the temperature rise of VIPV modules as a function of solar irradiation and wind speed are compared with experimental results. Based on analytical results for the temperature rise of VIPV modules, the potential of VIPV-EV to be deployed in 10 major cities worldwide is also analyzed. Although sunshine cities such as Phoenix show long annual driving range of 15,640 km in the case of no temperature rise of VIPV modules, the high reduction ratio of driving range with 17% due to temperature rise of VIPV modules is shown. Because the effects of wind speed are significant in Glasgow, power loss of VIPV-EV due to temperature rise of VIPV modules is only 2.2% by the

effects of wind. The effects of air-conditioner usage and partial shading in addition to the effects of temperature rise of VIPV modules are suggested as the other power losses of VIPV-EV.

This paper provides useful analytical results for the effects of solar irradiation, wind speed and temperature rise and radiative cooling of VIPV modules upon driving distance of VIPV-EV.

2. Analysis of Temperature Rise of PV Modules for VIPV Application

The conversion efficiency of PV modules is very sensitive to their temperature, and their output power decreases with the temperature rise of the modules. For VIPV applications requiring large amounts of electricity in a small surface area, heat dissipation of PV modules and development of low-temperature coefficient PV modules [8] based on analysis of temperature rise of PV modules under sunshine conditions are significant. The temperature of PV modules is increased with an increase in solar irradiation. Figure 1 shows the temperature rises of the Si module (black circle) [9] and GaAs module (blue square) [9] in the case of wind speed of 0.75 - 1.25 m/s and Si module [9] in the case of wind speed of 3 m/sec (red rectangular) as a function of solar irradiation. In the ref. 9, wind speed and direction were recorded using a cup anemometer, irradiance was obtained from both a thermopile pyranometer and silicon reference cell mounted in-plane with the modules, temperature readings for back-of-module, box interior, and car locations were obtained using T-type thermocouples. Following measurements have been carried out in the ref. 10: Module temperature measurements by using thermo couples connected to cell backside, solar irradiance measurements by using solar radiation intensity meters, wind speed measurements by using windmill-type wind vane anemometer, and ambient temperature measurements by using ventilation type temperature gage. Temperature rise differences between Si and GaAs modules are attributed mainly to the difference in module size [11] because small size GaAs module is thought to be effectively heat-dissipated.

Because our data for temperature rise of PV modules have been fitted by using the expression by King *et al.* [12], following expression for the temperature rise ΔT of PV modules was used in this study.

$$\Delta T = T_m - T_0 = G * e^{(a+b*v)} \quad (1)$$

where T_m is the module temperature [°C], T_0 is the ambient temperature [°C], G is the solar irradiation incident on the module surface [W/m^2], and v is the wind speed [m/s]. a is the empirically-determined coefficient establishing the upper limit for module temperature at low wind speed and high solar irradiation, and b is the empirically-determined coefficient establishing the rate at which module temperature decreases as wind speed increases.

The results for 3 cases calculated by using eq. (1), and parameters a and b shown in Table 1 are also shown in Figure 1. The measured results indicate that the module temperature depends on many parameters, such as solar irradiation,

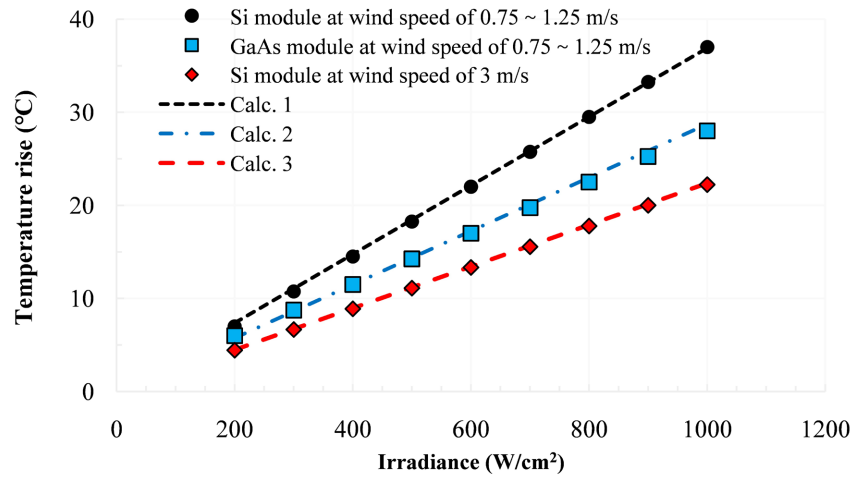


Figure 1. Temperature rise (measured temperature above ambient temperature) of Si module [9] and GaAs module [9] in the case of wind speed of 0.75 - 1.25 m/s and Si module [10] in the case of 3 m/s as a function of solar irradiation. The dotted lines are calculated values using eq. (1) and parameters a and b shown in Table 1.

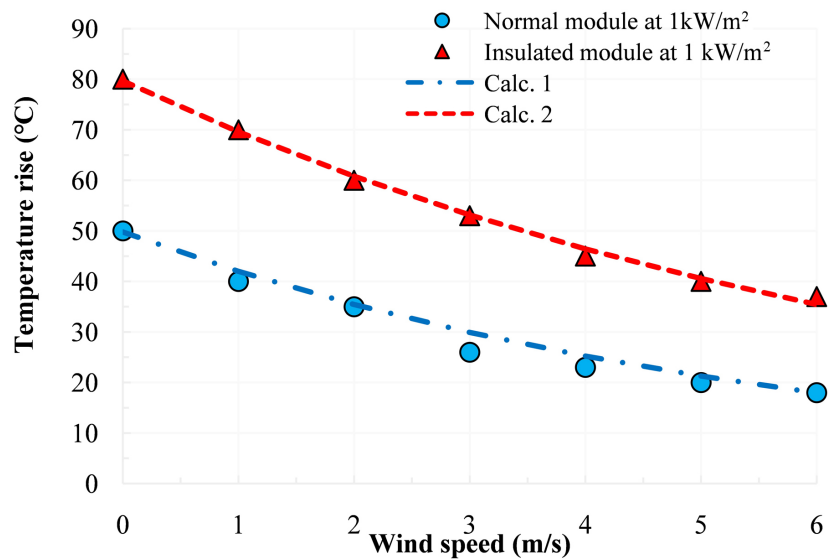


Figure 2. The temperature of PV modules is decreased with increased wind speed. The calculated temperature rise of crystalline Si solar cell modules with and without insulation as a function of wind speed.

wind speed, type and size of modules, and others (wind direction, module structure, module mounting configuration, shape and operating mode of car) as shown in Figure 1.

Figure 2 shows the calculated temperature rise [8] of crystalline Si solar cell modules with and without insulation under the solar irradiance of 1 kW/m² as a function of wind speed. It is clear from Figure 1 and Figure 2 that the temperature rise calculated by using eq. (1), and parameters a and b shown in Table 1 shows good agreement with measured values. If the back side of the modules is insulated, it restricts radiative and convective heat transfer from the back. Ac-

cording to Muller's simple model [13] to a common open-rack configuration shows that about half of the heat is exhausted from the front surface and half from the back surface with both radiative and convective terms being significant. If a module is insulated on the back, the insulation restricts both radiative and convective heat transfer to occur only out of the front of the module. It induces a more considerable temperature rise over the ambient, as shown in **Figure 2**. In the worst case, the PV module will show a temperature rise of 50 - 80°C, which causes a considerable reduction in the conversion efficiency.

Table 1 shows empirically-determined coefficients that are thought to be attributed to different module types and mounting configurations. Temperature rise differences from Si and GaAs modules are attributed mainly to the difference in module size [11] and the difference from coefficient b due to better heat dissipation in the case of GaAs solar cell modules, as shown in **Table 1**.

Table 1. Empirically determined coefficients for Si modules and GaAs modules shown in **Figure 1** and **Figure 2** and our Si modules to be shown in **Figure 3** and **Figure 4** were used to estimate module temperatures to be operated under various conditions as a function of solar irradiation, ambient temperature, and wind speed.

Module type	Mount	A	b	c	d	Reference
Si module (Fig. 1)	close mount	-3.05	-0.25	-	-	9
GaAs module (Fig. 1)	close mount	-3.05	-0.5	-	-	9
Si module under wind speed with 3 m/sec (Fig. 1)	close mount	-3.05	-0.25	-	-	10
Si module (Fig. 2)	Insulated Standard	-2.53	-0.135	-	-	10
Si module (Fig. 2)	(close mount)	-3	-0.17	-	-	10
Our recent Si module (Fig. 3)	Insulated	-2.7	-0.17	-9	-0.16	This study

3. Our Recent Studies on the Temperature Rise of PV Modules

The authors have measured the temperature of Si modules as a function of solar irradiance and wind speed in Miyazaki, Japan. The insulation material (Styrofoam board) was attached to the module back surface and it was blocked direct wind flow to the back surface.

Figure 3 shows the temperature rise ((module temperature) - (ambient temperature)) of PV modules versus solar irradiance in the 3 cases of average wind speed. The difference in temperature rise of PV modules was observed due to the thermal time constant. The thermal time constant is defined as the multiplication of heat capacity and thermal resistance. The PV module is generally heavy (-11 kg), and the heat capacity of it is relatively large. In addition, the thermal resistance of the car-mounted PV module in our experiment is higher than that of the general PV module because of the installation of the insulation material. The increasing wind speed increases the convective heat

transfer coefficient, then the thermal resistance decreases. As a result, the thermal time constant became short, and the difference in temperature rise was slight. Previously, the authors have also measured the module temperature under driving conditions [14]. The module temperature decreased from 23.4°C to 19.3°C due to the driving in the winter season (the ambient temperature during the experiment was 7.6°C). The wind speed (vehicle speed) is one of the significant factors for the module temperature of VIPV. We estimated the module temperature of VIPV incorporated in the passenger vehicle using the finite element method. As a result, for example, the average module temperature decreased due to the forced convection cooling by wind flow, and over 10 km/h in vehicle speed, the average module temperature was stable (as shown in supporting information).

The difference in temperature rise of PV modules characteristics of temperature rise in the morning. In the afternoon are different, as shown in **Figure 3**. In the morning, when solar irradiance of PV modules increases with time, the temperature rise of PV modules to compensate for module temperature under radiative cooling [15] [16] is thought to be delayed compared to increase in solar irradiance. In the afternoon, when the solar irradiance of PV modules decreases with time, the temperature decrease of PV modules is thought to be delayed compared to the decrease in solar irradiance because heat dissipation [16] from PV modules is thought to be late compared to decrease in solar irradiance. The difference in PV modules' temperature rise is reduced as wind speed increases, as shown in **Figure 3**.

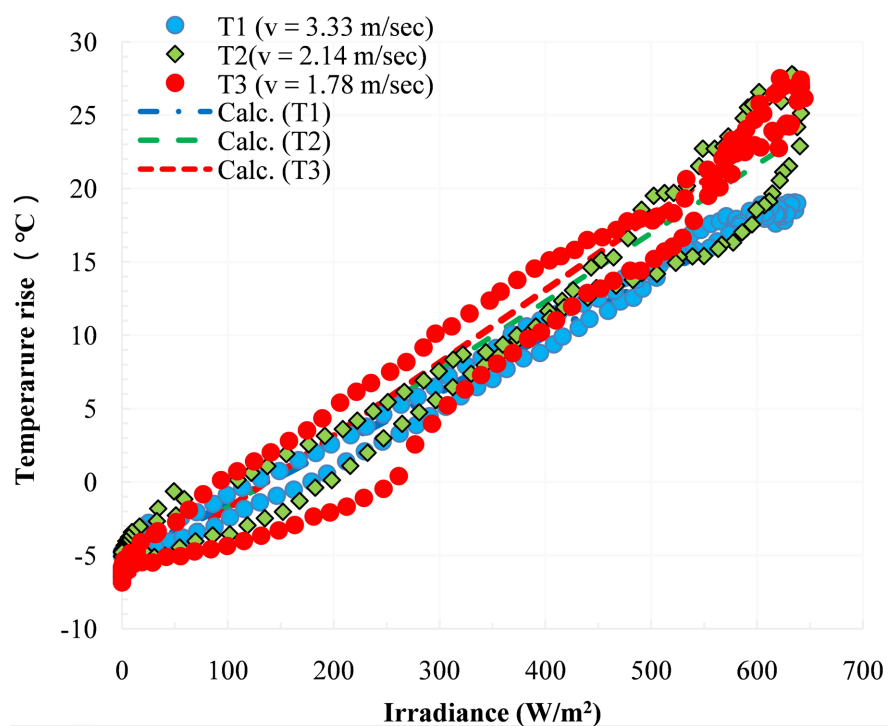


Figure 3. The temperature rise of solar cell modules versus solar irradiance in the 3 cases of average wind speed.

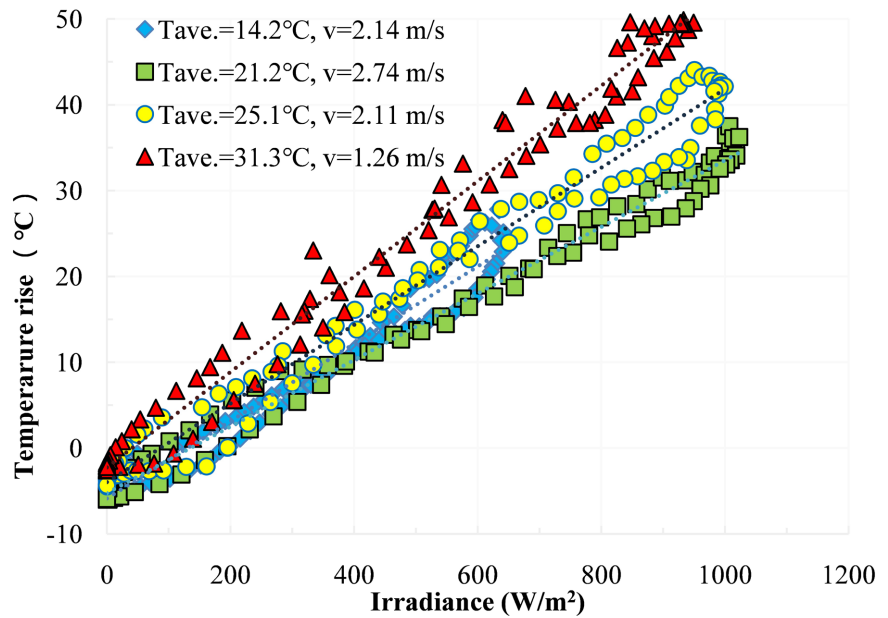


Figure 4. Temperature rise of solar cell modules versus solar irradiance in the 4 cases of average ambient temperatures.

In addition, it is shown in **Figure 3** that the temperature of PV modules is lower than the ambient temperature due to radiative cooling [15] [16] [17] [18] under low solar irradiance, especially at night. **Figure 4** shows the temperature rise of PV modules under zero solar irradiance ΔT_L in the nighttime at ambient temperature of around 4°C versus wind speed. In the region of zero solar irradiance, the temperature rise ΔT_L of PV modules is expressed by

$$\Delta T_L = T_m - T_0 = c * e^{(d*v)} = -9 * e^{(-0.16v)} \quad (2)$$

where c is the empirically-determined coefficient establishing the upper limit for module temperature decrease at low wind speed under zero solar irradiation, and d is the empirically-determined coefficient establishing the rate at which module temperature decreases as wind speed decreases. According to Zhu *et al.* [16], the temperature decrease of solar cells due to radiative cooling under zero solar irradiance and wind speed of 3 m/sec was simulated to be about 6°C, showing good agreement with the temperature decrease of 5.6°C estimated from eq. (2) for our solar cell modules due to radiative cooling.

Figure 4 shows the temperature rise of solar cell modules versus solar irradiance in the 4 cases of ambient temperatures. As shown in Fig. 4, the temperature rise of PV modules due to radiative cooling [21] [22] [23] [24] is dependent upon the ambient temperature. The higher ambient temperature shows less radiative cooling of PV modules.

Figure 5 and **Figure 6** show temperature rise ΔT relative to solar irradiance G of PV modules under normal solar irradiation conditions versus wind speed. Under solar irradiation, the temperature rise ΔT of PV modules is given by

$$\Delta T = G * e^{(a+b*v)} = G * e^{(-2.7 - 0.17v)} \quad (3)$$

Total temperature rise ΔT_T of PV modules by considering effects of ambient temperature T_0 is given by

$$\begin{aligned} \Delta T_T &= T_m - T_0 = \Delta T_L + \Delta T = 0.1844 * T_0 [^{\circ}\text{C}] + c * e^{(d*v)} + G * e^{(a+b*v)} \\ &= 0.1844 * T_0 - 9 * e^{(-0.16v)} + G * e^{(-2.7-0.17v)} \end{aligned} \quad (4)$$

In this study, empirically-determined coefficients a, b, c, and d determined are -2.7, -0.17, -9, and -0.16, respectively. It is clear in **Figure 3** that the wind speed also affect on radiative cooling of VIPV modules. Zhu *et al.* [16] have also pointed out effectiveness of radiative cooling of PV modules. In fact, good agreements between our results calculated by using eq. (4) (temperature rise of 37.7°C for wind speed v of 1m/s and 26.7°C for v of 3 m/s in the case of G = 800 W/m²) and results (temperature rise of 37°C for wind speed v of 1 m/s and 28°C for v of 3 m/s in the case of G = 800 W/m²) reported by Zhu *et al.* [16]. The first term of eq. (4) shows ambient temperature effects of radiative cooling of PV modules.

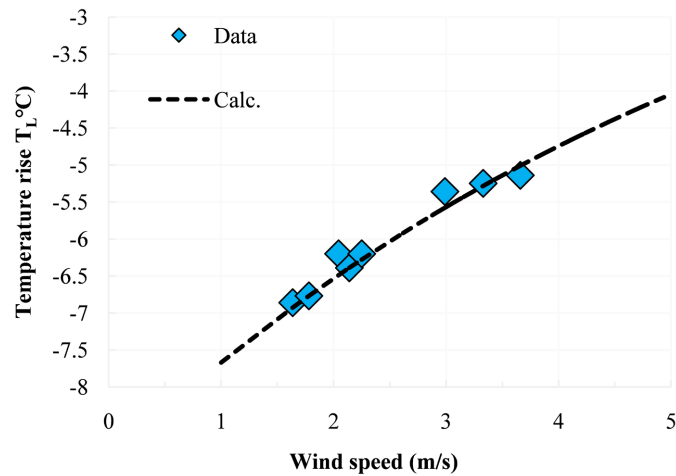


Figure 5. The temperature rise of PV modules under zero solar irradiance ΔT_L versus wind speed.

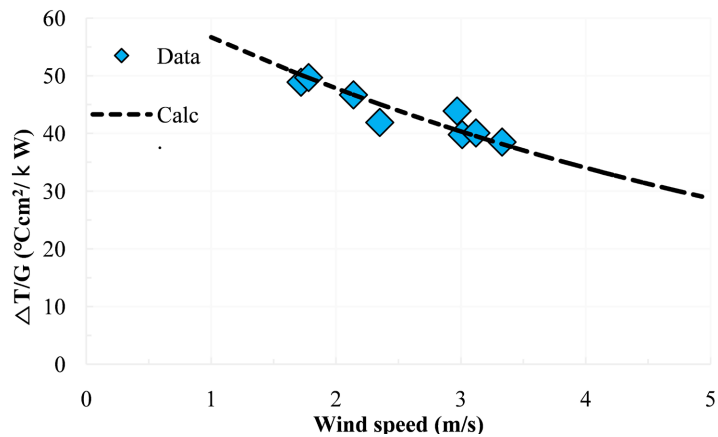


Figure 6. Temperature rise ΔT relative to solar irradiance G of solar cell modules under normal solar irradiation conditions versus wind speed.

Table 1 summarizes empirically-determined coefficients a , b , a and d for Si and GaAs modules shown in **Figure 1** and **Figure 2**, and our Si modules shown in **Figures 3-6**.

4. Analysis for Effects on Temperature Rise of PV Modules upon Driving Distance of VIPV-Powered Electric Vehicles

This study presents the effects of temperature rise of PV modules on the driving distance of VIPV-EV using the analytical procedure reported in our previous paper [8].

Figure 7 shows calculated results [8] for temperature coefficients TCs of crystalline Si, GaAs, and III-V compound dual-junction and triple-junction solar cells and modules as a function of its efficiencies compared with reported values [19]-[30] and estimated values. For example, the values of the temperature coefficients estimated from **Figure 7** are $-0.34\%/^{\circ}\text{C}$ and $-0.24\%/^{\circ}\text{C}$ for Si and GaAs modules [9] shown in **Figure 1** and $-0.4\%/^{\circ}\text{C}$ for Si modules [10] shown in **Figure 2**. Better temperature coefficients are expected for the cells with larger V_{oc} because the temperature sensitivity of V_{oc} dominates the performance sensitivity. The TCs of $-0.19\%/^{\circ}\text{C}$ and $-0.23\%/^{\circ}\text{C}$ are expected to be realized for InGaP/GaAs/InGaAs triple-junction solar cell modules with module efficiencies of 37% and 31.2%, respectively, though achieved values are $-0.333\%/^{\circ}\text{C}$ and $-0.337\%/^{\circ}\text{C}$ for 23.7% and 25.2% efficient InGaP/GaAs/Ge triple-junction solar cells. Possible TCs are estimated to be $-0.20\%/^{\circ}\text{C}$ for Si, $-0.14\%/^{\circ}\text{C}$ for GaAs, $-0.13\%/^{\circ}\text{C}$ for dual-junction, and $-0.14\%/^{\circ}\text{C}$ for triple-junction modules as shown in **Figure 7**.

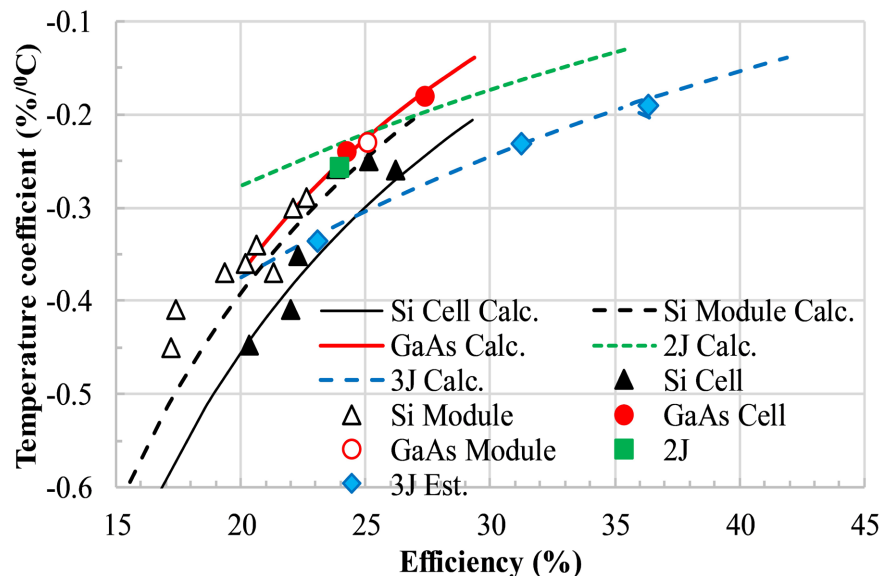


Figure 7. The higher efficiency PV modules show a better temperature coefficient. Calculated results for TCs of crystalline Si, GaAs, and III-V compound triple-junction cells and modules as a function of the conversion efficiencies of the cells and modules in comparison with reported values [19]-[30] and estimated values.

Table 2. Examples for efficiencies and temperature coefficients for and various solar cells and modules.

Solar cell, module	Structure	Efficiency (%)	Temperature Coefficient (%/°C)	Reference
Si cell	PERC	22.3	-0.35	24
	SHJ	25.1	-0.25	24
	Multi-crystal	17.2	-0.45	30
Si module	PERC	20.7	-0.36	30
	IBC	22.1	-0.3	26
	SHJ	22.5	-0.28	27
GaAs cell	LPE-grown heteroface	23.8	-0.258	25
	MOVPE-grown double hetero	22.6	-0.24	22
GaAs module	MOVPE-grown double hetero	27.4	-0.18	8
2-junction cell	MOVPE-grown GaInP/InGaAs	25.1	-0.23	8
	MOVPE-grown GaInP/InGaAs/Ge	24	-0.257	23
3-junction cell	MOVPE-grown GaInP/InGaAs	25.7	-0.337	23
	MOVPE-grown GaInP/InGaAs	31.3	-0.232	8
	MOVPE-grown GaInP/InGaAs	35.4	-0.191	8

PERC: passivated emitter rear contact, SHJ: Si hetero junction, IBC: interdigitated back contact, LPE: liquid phase epitaxy, MOVPE: metal organic vapor phase epitaxy.

Table 2 shows examples for efficiencies and temperature coefficients for and various solar cells and modules.

Although better temperature coefficient of less than $-0.2\%/^{\circ}\text{C}$ will be obtained with PV modules, as shown in **Figure 7**, the current temperature coefficient for Si modules is around $-0.30\%/^{\circ}\text{C}$ as shown **Table 2**. The following analysis used $-0.30\%/^{\circ}\text{C}$ as the temperature coefficient of PV modules.

The following equation calculated the daily driving distance (DD) of VIPV-EV:

$$\text{DD}[\text{km}/\text{day}] = G[\text{kWh}/\text{m}^2/\text{day}] * \text{SE} * \eta[\%] * (1 - \text{TC} * \Delta T) * A[\text{m}^2] * \text{EM}[\text{km}/\text{kWh}] \quad (5)$$

where G is the global solar irradiation, SE is the efficiency of the PV system (according to our previous study [31], 0.739 was used in this study), η is the efficiency of the PV module, TC is the temperature coefficient of PV module, ΔT is the temperature rise of PV module, A is the area of PV module, and EM is the electric mileage of the VIPV-EV. In the calculation, 1 kW was used as the output power of the VIVP module, and 10 km/kWh was assumed as EM .

Figure 8 shows world map, and data for ambient temperature [$^{\circ}\text{C}$] and daily average global solar irradiation G [$\text{kWh}/\text{m}^2/\text{day}$] taken from the references [32] [33] in the major cities in the world.

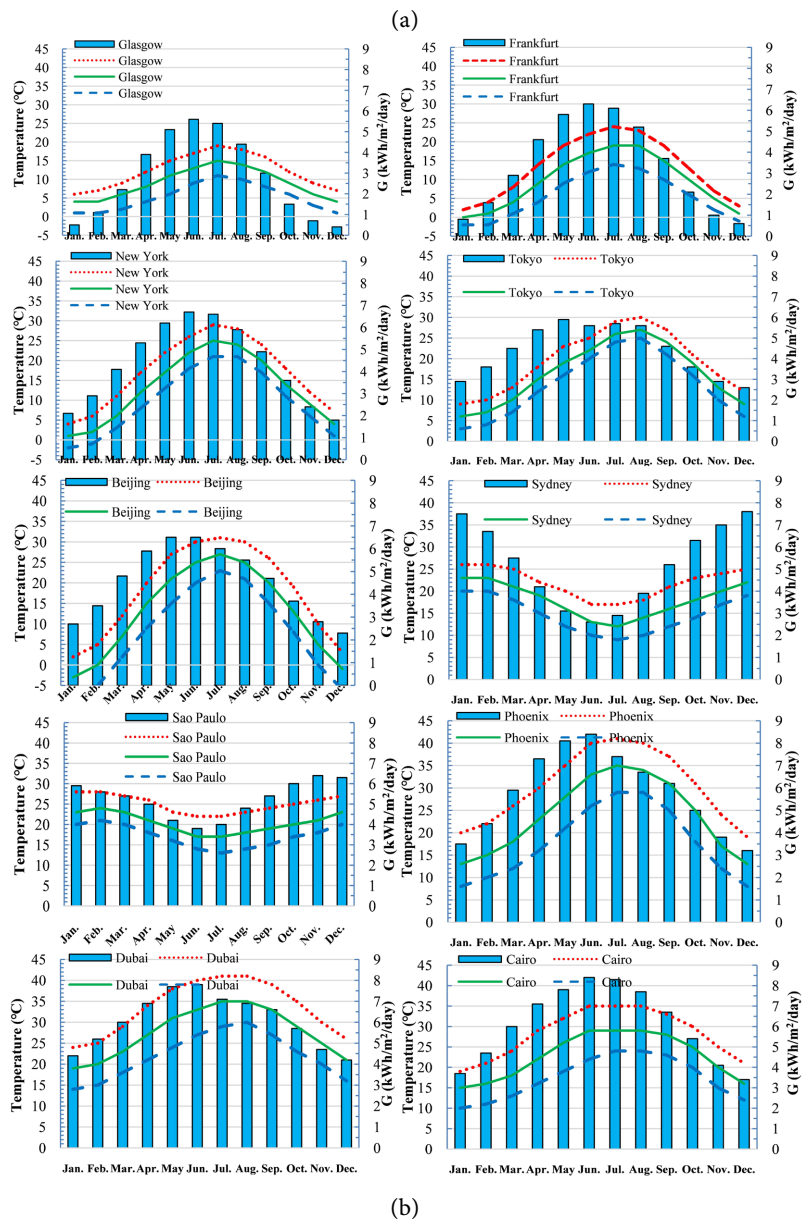


Figure 8. (a) World map, (b) daily average global solar irradiation G [$\text{kWh}/\text{m}^2/\text{day}$], and monthly maximum, average, and minimum ambient temperature [$^{\circ}\text{C}$] in the major cities in the world [32] [33].

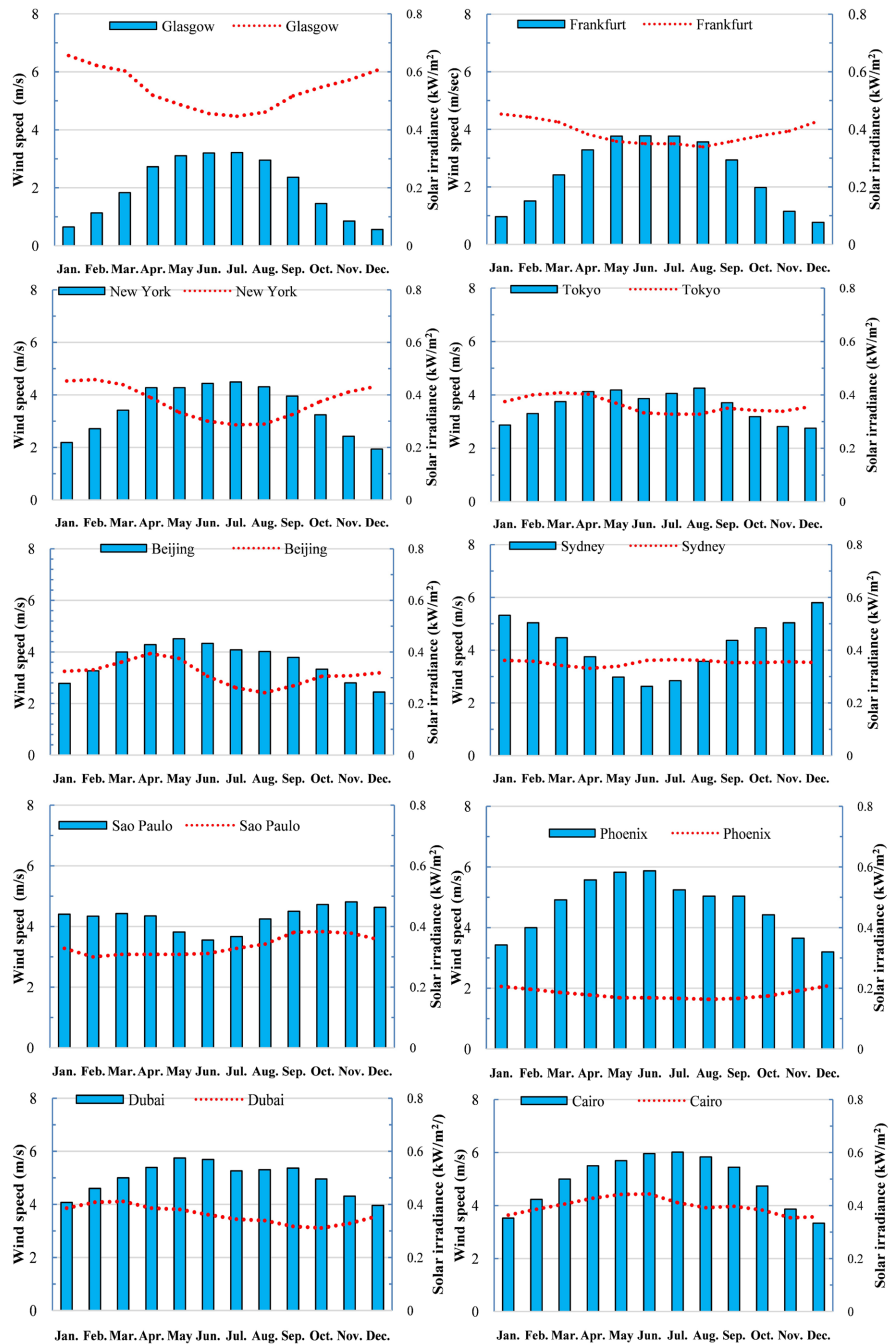


Figure 9. Average solar irradiance [kW/m^2] and average wind speed [m/s] in the major cities in the world [32] [33].

Figure 9 shows the average solar irradiance [kW/m^2] and average wind speed [m/s] taken from the references [32] [33] in the major cities in the world.

The temperature rise of VIPV modules was calculated in the cases of GaAs module, Si module, and module insulated by using eq. (1) and parameters shown in **Table 1**, and in the case of our Si module by using eq. (4) and parameters shown in **Table 1**, and assuming $-0.3\%/^{\circ}\text{C}$ as the temperature coefficient of VIPV modules.

Figure 10 shows annual driving distances calculated by using eq. (5) and by ignoring the effects of wind speed and by considering power loss due to the temperature rise of PV modules for VIPV-EV installed with 1 kW VIVP module and electric mileage EM of 10 km/kWh under driving in major cities in the world. Although sunshine cities such as Phoenix, Dubai, and Cairo show a more extended annual driving range with 15,600 - 16,400 km and in the case of ignoring the effects of temperature rise of VIPV modules, the high reduction ratio of driving range with 17% due to temperature rise of VIPV modules is estimated in the case of insulated modules. On the other hand, Sydney and Sao Paulo are thought to keep a more extended annual driving range of about 12,300 km by less reduction ratio of driving range with 12% even under the temperature rise of VIPV modules. Populous cities such as Tokyo, New York, and Beijing show an annual driving range of about 10,800 km by reduction ratio of driving range by about 9% even under a temperature rise of VIPV modules.

Figure 11 shows annual driving distances calculated by considering power loss due to the temperature rise of PV modules and the effects of wind speed for VIPV-EV installed with 1 kW VIVP module and EM of 10 km/kWh under driving in major cities in the world. It is clear that wind speed decreases the temperature rise of VIPV modules and increases the driving distance of VIPV-EV. Mainly because the effects of wind speed are significant in Glasgow, power loss of VIPV-EV decreases from 5.5% to 2.2% by the effects of wind speed. However, because of less wind speed in Phoenix, the power loss of PV-EV decreases from 17.1% to 14.3% by the effects of wind speed, and the power loss of PV-EV is still high. The power loss of PV-EV in Dubai and Cairo is still high (11.8%).

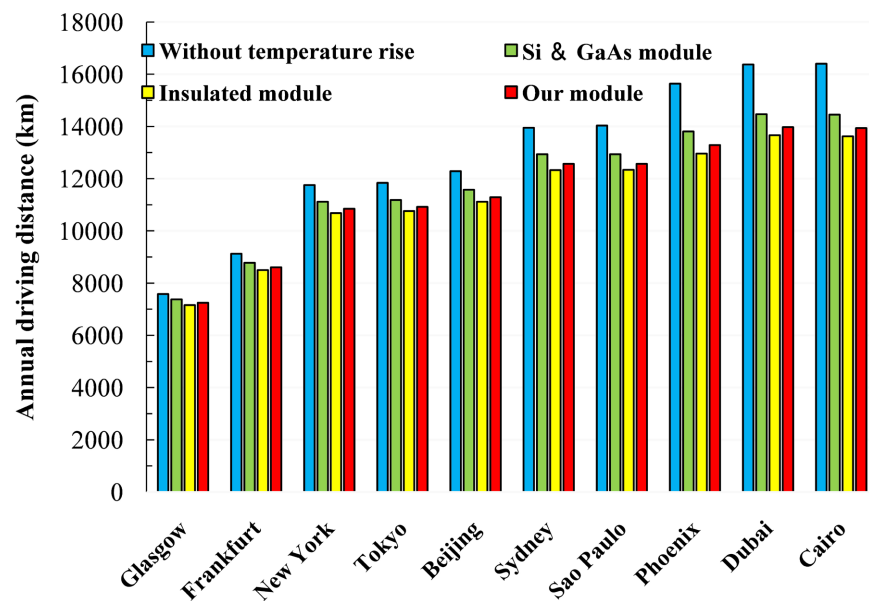


Figure 10. Annual driving distances calculated by ignoring the effects of wind speed and by considering power loss due to the temperature rise of PV modules for VIPV-EV installed with 1 kW VIVP module and EM of 10 km/kWh under driving in major cities in the world.

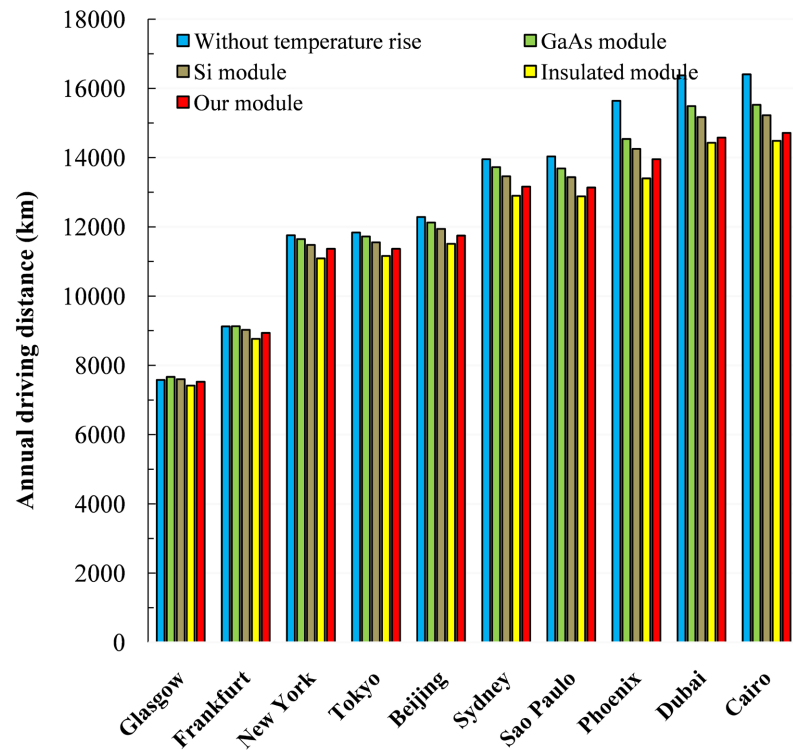


Figure 11. Annual driving distances calculated by considering power loss due to the temperature rise of PV modules and the effects of wind speed for VIPV-EV installed with 1 kW VIVP module and EM of 10 km/kWh under driving in major cities in the world.

On the other hand, Sydney and Sao Paulo are thought to keep a more extended annual driving range of about 12,900 km by less reduction ratio of driving range with about 8% even under the temperature rise of VIPV modules. Populous cities such as Tokyo, New York, and Beijing show an annual driving range of about 11,200 km with a reduction ratio of driving range by 6% even under a temperature rise of VIPV modules. In addition, it is shown in **Figure 10** and **Figure 11** that temperature rise behavior of our insulated Si solar cell modules is improved compared to the insulated Si solar cell modules reported by Wheeler *et al.* [9]. That is due to the effects of radiative cooling of PV solar cell modules.

As shown in **Figure 3**, a difference in the driving distance of VIPV-EV driving in the morning and the afternoon is expected due to the radiative cooling of PV modules. **Figure 12** shows annual driving distances estimated by considering power loss due to the temperature rise of PV modules and effects of wind speed for VIPV-EV installed with 1 kW VIVP module and EM of 10 km/kWh under driving in Tokyo in the morning and in the afternoon and average driving distance. It is suggested in **Figure 12** that a longer driving distance of VIPV-EV driving in the morning is expected compared to driving distance of VIPV-EV driving in the afternoon due to the radiative cooling of PV modules. The radiative cooling of PV modules significantly impacts the efficiency improvement of PV modules and expands the driving distance of VIPV-EV. According to

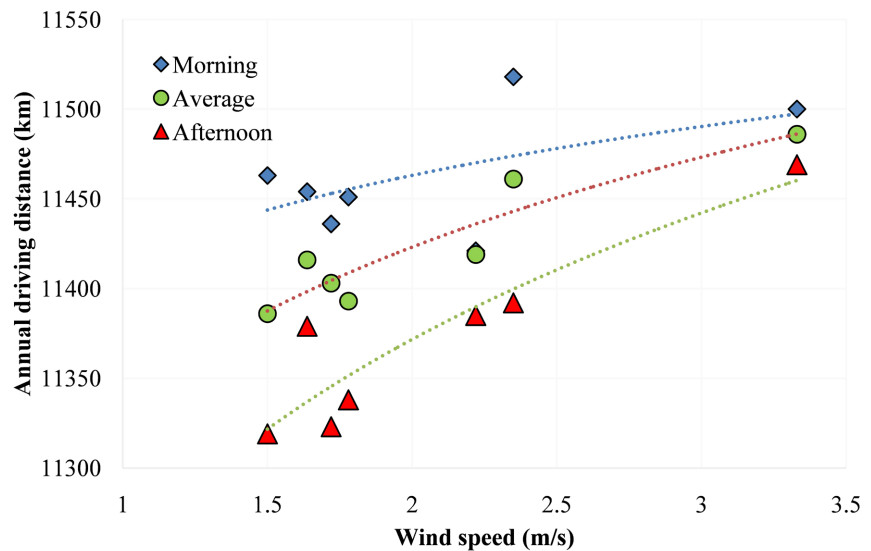


Figure 12. Annual driving distances estimated by considering power loss due to temperature rise of PV modules and effects of wind speed for VIPV-EV installed with 1 kW VIPV module and EM of 10 km/kWh under driving in Tokyo in the morning and the afternoon and average driving distance.

Muller's simple model [13] to a common open-rack configuration shows that about half of the heat is exhausted from the front surface and half from the back surface with both radiative and convective terms being significant. Therefore, radiative cooling of PV modules is thought to be useful for further reduction in temperature rise of PV modules by improvements in module materials and configuration, and installation.

5. Comments on Additional Losses for Toyota Prius and Nissan Van Demonstration Cars

Although a daily driving distance of 26.6 km/day has been estimated for the Toyota Prius demonstration car installed with a high-efficiency 3-junction module with a module efficiency of more than 30% in our previous paper [5], the actual driving range of VIPV-powered electric vehicles is shown to be lower (17.0 km/day [6]). Using the similar procedure described above, the effects of temperature rise of PV modules upon driving distance of Toyota Prius demonstration car (output power of 860 W and electric mileage EM of 9.35 km/kWh) and Nissan Van demonstration car (output power of 1,150 W and electric mileage EM of 6.6 km/kWh) were analyzed.

Table 3 shows annual driving ranges estimated by considering the effects of temperature rise of VIPV modules for the Toyota Prius and Nissan Van demonstration cars and the actual annual driving range measured. Suppose one does not consider the effects of temperature rise of VIPV modules. In that case, annual driving ranges of 9,718 km (26.6 km/day) and 9,054 km (24.8 km/day) are expected for Toyota Prius and Nissan Van demonstration cars. However, annual driving ranges of 9,114 km (25.0 km/day) and 8,502 km (23.3 km/day) were es-

timated considering the effects of the temperature rise of VIPV modules. However, actual driving ranges of 6,211 km (17.0 km/day) and 7,090 km (19.4 km/day) were measured for Toyota Prius and Nissan Van demonstration cars [6] [34] [35]. **Table 3** suggests additional power loss of 31.9% and 16.6% for the Toyota Prius and Nissan Van demonstration cars.

In general, passenger cars operate under usage of air-conditioning, cooling, and heating. As a result, the electric millage is thought to be decreased, and thus driving distance is shortened. The power consumption of the air-conditioner is changed dramatically depending on the outside temperature. Although the Toyota Prius demonstration car is under test driving, an average daily driving distance of 17.0 km/day at average solar irradiation of 4.0 kWh/m²/day has been demonstrated [6]. The average daily driving distance of 17.0 km/day is lower compared to estimated daily driving distance of 26.6 km/day. The effect of air-conditioner usage is thought to cause such a difference in addition to the effects of temperature rise of VIPV modules as shown in our previous paper [34].

The shading of the vehicle integrated photovoltaics (VIPV) shading has been reported [14] [36] [37] to depend on the sun's altitude, climate condition, location, and shading objects such as buildings and houses, trees, poles, and others, driving and parking conditions. Average irradiation losses by partial shading were reported to be 0.03 on the highway, 0.07 in the suburbs, 0.23 in the Urban, about 0.5 near tall buildings, and 0.07 - 0.57 in the parking [37]. Because the driving distance of VIPV-powered electric vehicles is thought to be decreased by partial shading, developing solar cell modules with low power loss under partial shading is necessary. Analytical studies on the effects of air-conditioners and partial shading on the driving distance of VIPV-powered electric vehicles are in progress.

Table 3. Annual driving ranges were estimated by considering the effects of temperature rise of VIPV modules for the Toyota Prius and Nissan Van demonstration cars and the actual annual driving range measured. (reproduced with permission Ref. 34 [Wiley], [2023])

Car	Location	Annual driving range (km)			Additional power loss
		Estimated range without temperature rise	Estimated range with temperature rise	Actual annual driving range	
Toyota Prius test car (VIPV power = 860W, EM = 9.35 km/kWh)	Nagoya	9,718	9,114	6,211	16.6%
Nissan Van test car (VIPV power = 1150 W, EM = 6.6 km/kWh)	Yokohama	9,054	8,502	7,090	31.9%

6. Summary

The development of VIPV-powered electric vehicles (VIPV-EV) significantly reduces CO₂ emissions from the transport sector to realize a decarbonized society. Although long-distance driving of VIPV-EV without electricity charging was expected in sunny regions, the driving distance of VIPV-EV was affected by climate conditions such as solar irradiation and temperature rise of PV modules. In this paper, analytical results for effects of climate conditions such as solar irradiation and temperature rise of PV modules were presented by using our test data for Toyota Prius and Nissan Van demonstration cars installed with high-efficiency InGaP/GaAs/InGaAs 3-junction modules with a module efficiency of more than 30%. The potential of VIPV-EV to be deployed in major cities worldwide was also analyzed. Sydney in Australia are thought to have more extended driving range even under high sunshine conditions. It was also shown in this paper that the difference between the driving distance of VIPV-EV driving in the morning and the afternoon is due to the radiative cooling of PV modules. In addition, the importance of heat dissipation of PV modules and the development of high-efficiency PV modules with better temperature coefficients was suggested. The effects of air-conditioner usage and partial shading in addition to the effects of temperature rise of VIPV modules were suggested as the other power losses of VIPV-EV.

This paper provides useful analytical results for the effects of solar irradiation, wind speed and temperature rise and radiative cooling of VIPV modules upon driving distance of VIPV-EV.

Acknowledgements

The authors sincerely thank to the New Energy and Industrial Technology Development Organization (NEDO) for supporting R&D, and to Mr. M. Yamazaki, Mr. K. Fukushima and Mr. K. Kiryu, NEDO, and members of Toyota Tech. Inst., Sharp Co., Toyota Motor Co., Nissan Motor Co., and Dr. K-H. Lee, former Toyota Tech. Inst., Prof. N. Yamada and Dr. D. Sato, Nagaoka Univ. Tech., Prof. T. Hirota, Waseda Univ., Dr. K. Komoto, Mizuho, Inf. Res. Inst., Dr. M. Tanaka, PVTEC, and members of the NEDO's PV-powered Vehicle Strategy Committee for their helpful discussion and for providing fruitful information.

Author Contributions

M.Y. led this project, M.Y., Y.O. and T.M analyzed effects of temperature rise of various solar cell modules in cooperation with C.T., A.T. and A.J., EC-JRC. T.T., Sharp, developed III-V solar cell modules, K.N., R.O., N.K. and Y.O., Toyota T.I., developed Si solar cell modules. Y.O., K.A. and K. N. Univ. Miyazaki, collected data for temperature rise of various solar cell modules. T.M., T.N., K.Y., K.O., T.M. and A.S., Toyota Motor, collected data for driving distance and temperature rise for Toyota Prius demonstration car. T.T., Y.T. and Y.Z., Nissan Motor, collected data for driving distance and temperature rise for Nissan Van

demonstration car. M.Y, Y.O. and T.M. wrote the manuscript, and all other authors provided feedback.

Conflicts of Interest

The authors declare no conflicts of interest regarding the publication of this paper.

References

- [1] NEDO (2018) Interim Report “PV-Powered Vehicle Strategy Committee”. <http://www.nedo.go.jp/english/index.html>
- [2] Rodriguez, A.S., De Santana, T., MacGill, I., Ekins-Daukes, N.J. and Reinders, A. (2019) A Feasibility Study of Solar PV-Powered Electric Cars Using an Interdisciplinary Modeling Approach for the Electricity Balance, CO₂ Emissions, and Economic Aspects: The Cases of the Netherlands, Norway, Brazil, and Australia. *Progress in Photovoltaics: Research and Applications*, **28**, 517-532. <https://doi.org/10.1002/pip.3202>
- [3] Yamaguchi, M., Masuda, T., Araki, K., Sato, D., Lee, K-H., Kojima, N., Takamoto, T., et al. (2020) Role of PV-Powered Vehicles in Low-Carbon Society and Some Approaches of High-Efficiency Solar Cell Modules for Cars. *Energy and Power Engineering*, **12**, 375-395. <https://doi.org/10.4236/epe.2020.126023>
- [4] Yamaguchi, M., Masuda, T., Nakado, T., Yamada, K., Okumura, K., Satou, A., et al. (2023) Analysis for Expansion of Driving Distance and CO₂ Emission Reduction of Photovoltaic-Powered Vehicles. *IEEE Journal of Photovoltaics*, **13**, 343-348. <https://doi.org/10.1109/JPHOTOV.2023.3242125>
- [5] Yamaguchi, M., Masuda, T., Araki, K., Sato, D., Lee, K-H., Kojima, N., et al. (2021) Development of High-Efficiency and Low-Cost Solar Cells for PV-Powered Vehicles Application. *Progress in Photovoltaics: Research and Applications*, **29**, 684-693. <https://doi.org/10.1002/pip.3343>
- [6] Masuda, T., Nakado, T., Yamaguchi, M., Takamoto, T., Nishioka, K. and Yamada, K. (2022) Public Road Tests of Toyota Prius Equipped with High Efficiency PV Modules with Output Power of 860 W. *Proceedings of the 49th IEEE Photovoltaic Specialists Conference*, Philadelphia, 5-10 June 2022, 263. <https://doi.org/10.1109/PVSC48317.2022.9938532>
- [7] Yamaguchi, M., Masuda, T., Tanimoto, T., Tomita, Y., Ota, Y., Thiel, C., et al. (2023) Analysis for Effects of Temperature Rise of Solar Cell Modules upon Driving Distance of Photovoltaics-Powered Vehicles. *Proceedings of the 50th IEEE Photovoltaic Specialists Conference*, San Juan, 11-16 June 2023, 1. <https://doi.org/10.1109/PVSC48320.2023.10359881>
- [8] Yamaguchi, M., Masuda, T., Araki, K., Ota, Y., Nishioka, K., Takamoto, T., et al. (2021) Analysis for Temperature Coefficient and Their Effect on Efficiency of Solar Cell Modules for Photovoltaics-Powered Vehicles. *Journal of Physics D: Applied Physics*, **54**, Article ID: 504002. <https://doi.org/10.1088/1361-6463/ac1ef8>
- [9] Wheeler, A., Leveille, M., Anton, I., Leilaoui, A. and Kurtz, S. (2019) Determining the Operating Temperature of Solar Panel on Vehicles. *Proceedings of the 47th IEEE Photovoltaic Specialists Conference*, Calgary, 15-21 June 2020, 894. <https://doi.org/10.1109/PVSC40753.2019.9311292>
- [10] Yukawa, M., Asaoka, M., Takahara, K., Ohshiro, T. and Kurokawa, K. (1996) Estimation of Photovoltaic Module Temperature Rise. *Trans. IEEJ Journal of Industry*

- Applications*, **116-B**, 1101-1110. (In Japanese)
https://doi.org/10.1541/ieeipes1990.116.9_1101
- [11] Wheeler, A., Leveille, M., Anton, I., Limpinsel, M. and Kurtz, S. (2019) Outdoor Performance of PV Technologies in Simulated Automotive Environments. *Proceedings of the 47th IEEE Photovoltaic Specialists Conference*, Calgary, 15 June-21 August 2020, 898. <https://doi.org/10.1109/PVSC40753.2019.8981352>
- [12] King, D.L., Boyson, W.E. and Kratochvill, J.A. (2004) Photovoltaic Array Performance Model, Sandia Report: SAND2004-3535. Sandia National Laboratories, Albuquerque. <https://www.semanticscholar.org/paper/sandia>
- [13] Muller, M., Marion, B. and Rodriguez, J. (2012) Evaluating the IEC 61215 Ed.3 NMOT Procedure against the Existing NOCT Procedure with PV Modules in a Side-by-Side Configuration. *Proceedings of the 38th IEEE Photovoltaic Specialists Conference*, Austin, 3-8 June 2012, 697. <https://doi.org/10.1109/PVSC.2012.6317705>
- [14] Ota, Y., Araki, K., Nagaoka, A. and Nishioka, K. (2021) Evaluating the Output of a Car-Mounted Photovoltaic Module under Driving Conditions. *IEEE Journal of Photovoltaics*, **11**, 1299-1304. <https://doi.org/10.1109/JPHOTOV.2021.3087748>
- [15] Nishikawa, S. (1997) Characteristics of PV Cell Temperature and Cooling Effects on a Stand-Off Type PV Array. *Journal of Japan Solar Energy Society*, **23**, 52. (In Japanese)
- [16] Zhu, I., Raman, A., Wang, K.X., Anoma, M.A. and Fang, S. (2014) Radiative Cooling of Solar Cells. *Optica*, **1**, 32-38. <https://doi.org/10.1364/OPTICA.1.000032>
- [17] Sato, D. and Yamada, N. (2019) Review of Photovoltaic Module Cooling Methods and Performance Evaluation of the Radiative Cooling Method. *Renewable and Sustainable Energy Review*, **104**, 151-166. <https://doi.org/10.1016/j.rser.2018.12.051>
- [18] Li, Z., Ahmed, S. and Ma, T. (2021) Investigating the Effect of Radiative Cooling on the Operating Temperature of Photovoltaic Modules. *Solar RRL*, **5**, Article ID: 2000735. <https://doi.org/10.1002/solr.202000735>
- [19] Fan, J.C.C. (1986) Theoretical Temperature Dependence of Solar Cell Parameters. *Solar Cells*, **17**, 309-315. [https://doi.org/10.1016/0379-6787\(86\)90020-7](https://doi.org/10.1016/0379-6787(86)90020-7)
- [20] Abderrezek, M., Fathi, M., Mekhilef, S. and Djahli, F. (2015) Effects of Temperature on the GaInP/GaAs Tandem Solar Cell Performances. *International Journal of Renewable Energy Research*, **5**, 629-634.
<https://www.researchgate.net/publication/279915931>
- [21] Dupre, O., Vaillon, R. and Green, M.A. (2015) Physics of the Temperature Coefficients of Solar Cells. *Solar Energy Materials and Solar Cells*, **140**, 92-100.
<https://doi.org/10.1016/j.solmat.2015.03.025>
- [22] Yoshida, S. (1983) Study on Development of High Performance and Highly Reliable (AlGa)As/GaAs Solar Cells. PhD Thesis, Tokyo Inst. Tech., Tokyo. (In Japanese)
<https://topics.libra.titech.ac.jp/recordid/catalog.bib/1000262268>
- [23] Siefer, G. and Bett, A.W. (2014) Analysis of Temperature Coefficients for III-V Multi-Junction Concentrator Cells. *Progress in Photovoltaics: Research and Applications*, **22**, 515-524. <https://doi.org/10.1002/pip.2285>
- [24] Hishikawa, Y., Doi, T., Yamagoe, K., Ohshima, H., Takenouchi, T. and Yoshita, M. (2018) Voltage-Dependent Temperature Coefficient of the I-V Curves of Crystalline Silicon Photovoltaic Modules. *IEEE Journal of Photovoltaics*, **8**, 48-53.
<https://doi.org/10.1109/JPHOTOV.2017.2766529>
- [25] Panasonic. <https://news.panasonic.com>
- [26] SunPower. <https://www.enfsolar.com> <https://www.sisolar.co.jp>

- [27] Longi. <https://www.sisolar.co.jp>
- [28] Canadian Solar. <https://www.canadiansolar.com>
- [29] JA Solar. <https://www.jasolar.com>
- [30] Trina Solar. <https://www.trinasolar.com>
- [31] Masuda, T., Araki, K., Okumura, K., Urabe, S., Kudo, Y., Kimura, K., Nakado, T., Sato, A. and Yamaguchi, M. (2017) Static Concentrator Photovoltaics for Automotive Applications. *Solar Energy*, **46**, 523-531. <https://doi.org/10.1016/j.solener.2017.03.028>
- [32] Thiel, C., Amillo, A.G., Tansini, A., Tsakalidis, A., Fontaras, G., Dunlop, E., et al. (2022) Impact of Climatic Conditions on Prospects for Integrated Photovoltaics in Electric Vehicles. *Renewable and Sustainable Energy Review*, **158**, Article ID: 112109. <https://doi.org/10.1016/j.rser.2022.112109>
- [33] Weatherspark. <https://ja.weatherspark.com/>
- [34] Yamaguchi, M., Nakamura, K., Ozaki, R., Kojima, N., Ohshita, Y., Masuda, T., et al. (2023) Analysis of Climate Conditions upon Driving Distance of Vehicle Integrated Photovoltaics-Powered Vehicles. *Energy Technology*, **12**, Article ID: 2300692. <https://doi.org/10.1002/ente.202300692>
- [35] Tanimoto, T. (2022) Demonstration Test of EV Equipped with a Solar Power Generation System That Utilizes Solar Energy for Driving. *The 33rd International Photovoltaic Science and Engineering Conference (PVSEC-33)*, Nagoya, 14-17 2022 November, ThO-22c-01.
- [36] Tomita, Y., Saito, M., Nagai, Y., Zushi, Y., Tanimoto, T. and Nishijima, K. (2021) Development of Electric Vehicle with a High Power Photovoltaic System. *5th International Electric Vehicle Technology Conference (EVTech)*, No. 20214307.
- [37] Hirota, T., Kim, Y., Kobayashi, K., Kamiya, Y., Maeshima, S. and Komoto, K. (2022) Feasibility Study of Onboard PV for Passenger Vehicle Application (Second Report)—Influence of Vehicle Irradiation on Energy Balance of PV Generation and EV Energy Consumption. *Transactions of Society of Automotive Engineers of Japan*, **53**, 784-789. (In Japanese)